ORIGINAL PAPER

Macroscopic mixer for disparate property liquid–liquid mixing in aqueous sanitizer preparation

R. M. Ohol[1] · B. Vasuki[1]

Abstract

The present study introduces an active macroscopic mixing device for aqueous sanitizer preparation. It operates on a piezo-electrically actuated oscillating cantilever beam appropriate for disparate feature liquid–liquid mixing. A piezoelectric actu-ated cantilever beam at the third bending mode vibration frequency produces extreme vibrations when excited by a suitable voltage. Potent mixing occurs as the robust vibration energy is sent from the beam to the container's test liquid. In this work, different glycerol concentrations were mixed with deionized (DI) water and ethanol at 25 ℃. The mixer's performance to mix DI water–glycerol, ethanol–glycerol, and DI water–ethanol–glycerol considered a sanitizer was tested. The sanitizer mixture's measured density, viscosity, and surface tension values were 0.7502 g cm^{-3}, 1.8906 cp, 34.7893 dyne cm^{-1}, respectively. The measured aqueous-based glycerol mixture's density and viscosity values were validated with the computed values by previous researcher's models and formulas. The observed density reading of the aqueous-based 25% glycerol concentration mixture agreed with the estimated value of a density model having ± 1.1290% deviation.

Keywords Density · Oscillating cantilever beam · Piezoelectric · Surface tension · Viscosity

Introduction

Following the COVID-19 pandemic, continuous cleaning of hands is recommended using a hand-rub-based sanitizer for virus disinfection. The sanitizer preparation formulation suggests mixing of appropriate proportions of significant ingredients, distilled water, glycerol, and ethanol (Lee et al. 2020; Center for Drug Evaluation and Research 2020). Mixing is a process where solid, liquid, or gas molecules of a solution are in motion, moving from one location to another in a tank, chamber, or pipeline. Mixing methods are categorized as liquid–liquid, solid–liquid, gas–liquid, or a combination of all states such as solid–liquid–gas (Ohol and Vasuki 2020). The mixing process is completed when the solution becomes homogeneous or uniform, and non-uniformity in any form such as temperature, phase, concentration, colour, and viscosity are dispelled (Bowler et al. 2020). The essential governing aspects that decide the solution's uniformity for any general mixing method include fluid circulation type, stirring speed, the power required for operation, interfacial area, and mixing time.

Liquid–liquid mixing is a substantial operation in the food process, chemical, pharmaceutical, cosmetic industries, and clinical laboratories (Aubin 2019; Kozic et al. 2016). The mixing of honey and sugar syrup in the food processing unit is necessary to prepare emulsion, creams, soups, sauces, mayonnaise, and margarine (Cullen 2009). Similarly, in the dairy industry to prepare butter from the cream and the mixing of milk proteins and fat in a liquid such as water for the preparation of homogenized milk (Elia et al. 2011). Processing of different densities and viscosities liquids is a challenge for the cosmetics industry (Ghotli et al. 2013). The cosmetics and personal care products manufacturing unit comprises flawlessly mixing of fragrances, glycerine, rose water, proteins, conditioners, dyes, colours, thickeners, vitamins, preservatives, and gels to prepare thin lotion, cream, and emulsion at a small to medium scale (Sharma et al. 2018). An example is the preparation of aloe vera gel from the naturally occurring aloe vera juice. In the pharmaceutical industry, liquid–liquid mixing is a significant phenomenon in which an accurate measure of drug mixing is substantial (Dickey 2012). In the production of liquid

✉ R. M. Ohol
 icers2019@gmail.com

1 Department of Instrumentation and Control Engineering,
 National Institute of Technology, Tiruchirappalli,
 Tamil Nadu 620015, India

medicine suspensions, improper shaking methods will result in inadequate mixing, which will ensure a lack of dosage homogeneity.

DI water, ethanol, and glycerol are solvents frequently used in the industries mentioned above. While the blending of mixable liquids happens naturally by molecular diffusion and convection, it is not sufficient and time-consuming (Williams et al. 2009). Hence, fluidic mixing devices are significant; these are categorized based on channel size as microfluidic, macroscopic, and large-scale mixing devices (Aubin et al. 2010). In micromixing, mixing happens on a molecular scale (Vilardi and Verdone 2020). The fluid's mixing rate and mass transfer depend on the type of flow existing on a rotating body surface (Vilardi et al. 2020). Microfluidic mixing devices are classified as passive and active mixers (Hessel et al. 2005; Bayareh et al. 2020). Passive mixers are easy to implement compared to active mixers (Rahbarshahlan et al. 2020). Active mixers consist of more moving parts and hence, are more challenging to implement. But active mixers can produce outstanding mixing performance than that of passive mixers (Cai et al. 2017). Besides simple construction and a static mode of operation, some restraints limit passive microfluidic mixer applications. They are channel blockage, high-pressure drops, and bounded flow capacity. Researchers evaluated the performance of passive mixers for the mixing of the same property fluids and not for viscous and disparate property fluids, thus, restricting their application for viscous fluid mixing (Rampalli et al. 2020; Das et al. 2017).

Macroscopic mixing devices are sufficiently large and where the mixing process is visible to the naked eye, devoid of any optical magnifying device. Large-scale stirred tank mixers in chemical industries deal with a massive amount of fluid mixing and are not suitable for a lesser amount of fluids (Zhang and Chen 2008). Also, macroscopic mixing devices beat the limitations of microfluidic mixing devices such as progressive flow, low pressure drops, lack of channel blockage, and multi-gram sample preparation efficacy (Wegner et al. 2011). In general, the most mixing devices reported in the literature work on the rotational movement of the fluid around a shaft or disc (Vilardi et al. 2019). If the entire liquid moves in a circular motion, no collision occurs among the liquid's molecules (Mashimo 2013). Additionally, the speed of the liquid molecules is high near the rotating body and less at the tank's internal wall (Lu et al. 2002). Hence, no appropriate mixing occurs on the inner side of the tank wall.

The study of fluid-based unit's motion and numerous forces acting on them is an interesting area (Mallinson et al. 2016). More than fifty percent of the investigation on the fluid's attributes incorporates density and viscosity measurements collectively. The most experimental viscous fluid flow studies utilize aqueous glycerol solutions and knowledge of fluid viscosity plays a significant role in such studies

(Shankar and Kumar 1994; Segur and Oderstar 1951). Equally, the density of aqueous glycerol solution differs as the concentration of glycerol changes. Nian-Sheng Cheng developed a formula for aqueous glycerol solution's viscosity (Cheng 2008).

Similarly, Andreas Volk and Christian J. Kahler created a density model for an aqueous glycerol solution (Volk and Kähler 2018). The other significant considerations related to fluid properties are surface tension and the refractive index (Takamura et al. 2012; Alkindi et al. 2008; Chenlo et al. 2004; Cristancho et al. 2011; Nakagawa and Oyama 2019). Due to surface tension, the fluid behaves like an extended layer, allowing bonding between fluid molecules and acting as a wall between external items and the liquid. The surface tension of water is high, and so, it does not clean the hands effectively when used alone. An apt proportion of ethanol and glycerol mixed with water reduces the surface tension of water, and so, the mixture disinfects the hands. Also, the refractive index measurement of the mixed solution correctly monitors its concentration (Zhu et al. 2003).

This paper presents the development of a novel macroscopic active mixer for disparate liquid–liquid mixing of different glycerol concentrations in aqueous and alcoholic solutions. Active mixing techniques have proved to work well as compared to a passive mixer. In the proposed method, vibrating mode frequency is utilized as a tool for liquid–liquid mixing. The viscous fluid's influential circulation occurs vigorously in all directions—vertical and horizontal. All the liquid molecules are in strong motion; hence, dispersion of fluid occurs naturally everywhere. Thus, potent mixing occurs, even at the tank's inner sidewall, and overcomes the limitations of a conventional rotational mixer. The mixer can actuate on demand and have a mode selection facility for a particular application. Similarly, it can substitute existing mixers on a laboratory scale. To the best of our knowledge, a piezoelectrically actuated vibrating cantilever beam-based active macroscopic mixer for disparate liquid–liquid mixing has not been widely reported in the literature. The mixer is adequate for aqueous sanitizer preparation, food processing, dairy, cosmetics, and pharmaceutical unit.

Materials and methods

Chemicals

To mix different property fluids, glycerol was used as a viscous fluid. Glycerol is inexpensive, non-toxic both to the environment and human health, free from harm and hence is used for experimentation. The proposed mixer mixed different concentrations of glycerol 10, 25, 50, 75, and 90% by volume in solvents, DI water, and ethanol, respectively. Similarly, a sanitizer solution was prepared comprising DI

water–ethanol-10% of glycerol. Table 1 shows the comprehensive physical and chemical properties of the chemicals.

Method followed for the disparate liquid–liquid mixing

This study emphasizes liquid–liquid mixing of different physical and chemical properties such as aqueous–viscous, alcoholic–viscous, and aqueous–alcoholic–viscous liquids. Table 2 and Section I illustrate glycerol concentration in terms of mass and volume. Sections II–VI indicate the proposed methodology for mixing solvents. *M* represents the mixed solution. However, each mixing reading considered a total of 25 ml volume and glycerol concentration by % of volume. A stopwatch measured mixing time and depending on the liquid's property, such as viscosity. The present work evaluates the mixture's mixing performance, as mentioned in Table 2 and Sections II–IV, by measuring the density, viscosity, and surface tension and refractive index of the aqueous glycerol mixture.

Additionally, for mixing evaluation analysis, a UV–visible spectrophotometer measured the mixture's absorbance values as shown in Table 2 and Sections V and VI (Nogueira et al. 2019). A Gas Chromatography-Mass Spectrometer (GCMS) measured the GCMS spectrum of the *M-17* mixture.

Schematic representation and design of the proposed disparate liquid–liquid mixing system

Figure 1a is a schematic representation of the proposed disparate liquid–liquid mixing arrangement. A piezoelectric patch was glued to an Aluminium cantilever beam's surface, and the beam along with the patch acted as a piezoelectric actuated cantilever beam. A metal stand was used to fix the piezoelectric actuated cantilever beam at one end, with the free end being dipped in the mixing tank containing the test liquid. The mixing tank was made of borosilicate glass, of 50 ml volume, with 25 ml test liquid corresponding to a height of 27 mm. The test fluid contained DI water and different glycerol concentrations, ethanol, discrete glycerol's concentration, or even DI water, ethanol, and 10% glycerol. Figure 1b indicates the test fluid consisting of DI water and 50% glycerol concentration and their corresponding heights for a total volume of 25 ml at rest.

Further, DI water was indicated as a coloured liquid to differentiate between DI water and glycerol. A function generator (Scientific, Model: SM 5074) in aggregation with a high-voltage amplifier (TRek, Model 10/10 B) supplied the input voltage for the piezoelectric patch's actuation. As the piezoelectric activated cantilever beam was stimulated by an appropriate excitation voltage, it started oscillating. Subsequently, the oscillating beam's vibration energy was sent to the container's test fluid, and mixing started.

In the present study, the piezoelectric activated beam was operated at the third bending mode vibration frequency as the beam vibrated powerfully in this mode. Simultaneously, the beam's insertion depth in the test fluid was taken as 5 mm as the fluid's drag force was minimum at this height and caused the utmost mixing. The laser displacement sensor (KEYENCEL-100 Intelligent-L) measured the deflection of the beam's free end, and a DAQ card (USB-1408FS-Plus) logged the data.

A stopwatch was used to measure the time required for mixing, which depended on the solvent type and the glycerol concentration used. The present methodology measured the mixture's density, viscosity, surface tension, refractive index, absorbance, while the GCMS spectrum evaluated the solution's mixing performance. A specific gravity bottle measured the mixture's density, An Ostwald's viscometer measured viscosity, a stalagmometer

Table 1 Comprehensive physical and chemical properties of the chemicals

Dye/solvent	Unit	Glycerol	DI water	Ethanol	Methyl red dye powder
Appearance	–	Colourless, odourless, viscous fluid	Aqueous solvent, colourless fluid	Alcoholic solvent, colourless fluid, analytical grade	Deep red powder
Solubility	–	Miscible in water and ethanol	–	Assay by volume 99.9% maximum	Soluble in water, ethanol
Molecular weight	g mol^{-1}	92.09	18.02	46.07	269.31
Density	g cm^{-3}	1.26	0.997	0.789	1.31
Viscosity	cp	1412	0.890	1.074	–
Surface tension	dyne cm^{-1}	63.472	72.2	21.97	–
Maximum absorptivity λ_{max}	nm	270	–	–	410
Refractive index	–	1.474	1.333	1.361	–

Table 2 Glycerol concentration and different mixtures preparation by the proposed methodology

		10	25	50	75	90
I – Glycerol concentration in terms of volume and mass						
Glycerol	%	10	25	50	75	90
Quantity	ml	2.5	6.25	12.5	18.75	22.5
Mass	g	2.8349	5.6699	17.0097	22.6796	26.9319
II – Aqueous–glycerol's 10, 25, 50, 75, 90% concentration mixture						
DI water	(A)ml	22.5	18.75	12.5	6.25	2.5
Glycerol	(C)ml	2.5	6.25	12.5	18.75	22.5
Mixture	(A+C)ml	M-1	M-2	M-3	M-4	M-5
III – Ethanol–glycerol's 10, 25, 50, 75, 90% concentration mixture						
Ethanol	(B)ml	22.5	18.75	12.5	6.25	2.5
Glycerol	(C)ml	2.5	6.25	12.5	18.75	22.5
Mixture	(B+C)ml	M-6	M-7	M-8	M-9	M-10
IV – Aqueous–Ethanol–10% glycerol (Sanitizer) M-11 mixture						
Mixture	M-11	ml	DI water (11.25 ml)+ethanol (11.25 ml)+glycerol (2.5 ml)			
V – Aqueous methyl red dye solution (10 mg l^{-1}) – glycerol's 10, 25, 50, 75, 90% concentration mixture						
Aqueous methyl red dye solution 10 mg l^{-1} (sol-1)	(D) ml	22.5	18.75	12.5	6.25	2.5
Glycerol	(C) ml	2.5	6.25	12.5	18.75	22.5
Mixture	(D+C)ml	M-12	M-13	M-14	M-15	M-16
VI – Alcoholic methyl red dye solution (10 mg l^{-1})– glycerol's 10, 25, 50, 75, 90% concentration mixture						
Alcoholic methyl red dye solution 10 mg l^{-1} (sol-2)	(E)ml	22.5	18.75	12.5	6.25	2.5
Glycerol	(C)ml	2.5	6.25	12.5	18.75	22.5
Mixture	(E+C)ml	M-17	M-18	M-19	M-20	M-21

Fig. 1 a Schematic representation of the proposed disparate liquid–liquid mixing arrangement **b** Mixing tank with DI water and 50% glycerol concentration at rest
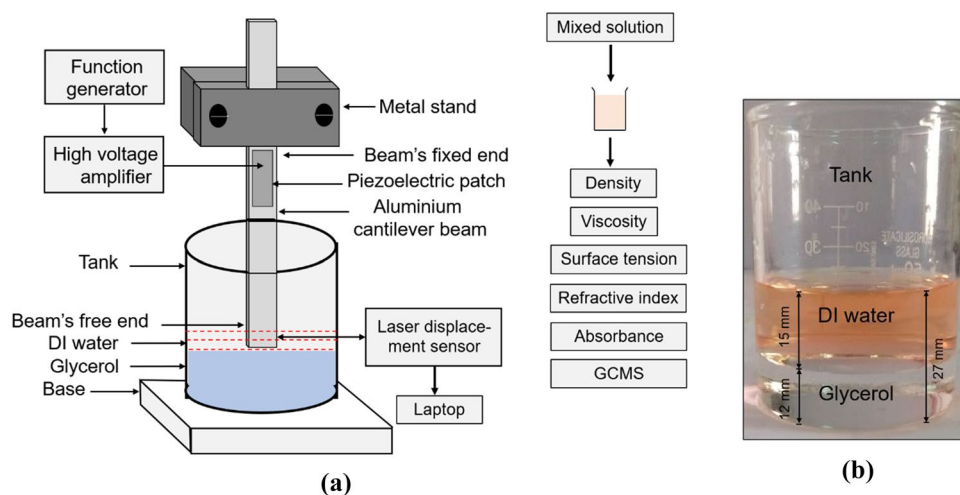
the surface tension, and refractive index the formula. A UV–visible spectrophotometer (LAB INDIA UV 3092) measured the mixture's absorbance values, and GCMS (Bruker 45X-GC) produced the GCMS spectrums.

The piezoelectric actuated cantilever beam

A piezoelectric patch was pasted on the Aluminium beam's surface and the beam along with the patch acted

as a piezoelectric activated cantilever beam as indicated in Fig. 1a. The cantilever beam was of Aluminium grade-6061, which has high strength and excellent corrosion resistance. The selected beam's width was such that a wide range of fluid in the tank was in contact with the vibrating mass. The Aluminium cantilever beam's structural sizes and properties were length 200 mm (l_b), width 15 mm (w_b), thickness 0.5 mm (t_b), density 2700 kg m^{-3} (ρ_b), and Young's modulus 68.9 GPa (E_b).

A piezoelectric patch of -SP-5H grade (Make-Sparkler Ceramics Pvt. Ltd., India) was pasted on the cantilever beam's surface using Araldite (AV138M) epoxy resin. The piezoelectric patch's dimensions and material properties were length 76.2 mm (l_p), width 12.7 mm (w_p), thickness 0.5 mm (t_p), density 7500 kg m^{-3} (ρ_p), Young's modulus 47.62 GPa (E_p), and piezoelectric constant -265×10^{-12} C/N (d_{31}).

Analytical modelling and analysis

Piezoelectric actuated cantilever beam's exerted force and the test fluid's viscous drag force

For a piezoelectric actuated cantilever beam inserted in the test liquid, two forces are substantial. The first force is the piezoelectric actuator's exerted force, and the other relates to the test fluid's drag force (Shih et al. 2001; Zhang et al. 2019). In this study, the magnitude of the piezoelectric actuator's force was enormous compared to the fluid's drag force, which resulted in the potent mixing of the viscous liquid. A piezoelectric actuated cantilever beam exerted a force F_p, expressed by the equation

$$F_p = \frac{M_p}{b} \tag{1}$$

where M_p is the effective mass of the piezoelectric patch, and b the distance between the beam's fixed end and patch's centre as indicated in Fig. 2a.

$M_p = w_p \times E_p \times d_{31} \times V \times l$ and $b = \frac{l_p}{2} + l$, where l is the distance between the beam's fixed end and patch's starting point, V excitation voltage for the piezoelectric patch, and other terms as expressed in Section the piezoelectric actuated cantilever beam.

The cantilever beam's effectual mass M_b at the piezoelectric patch's end and the Aluminium segment is expressed as

$$M_b = 0.236\left(E_p \times t_p \times E_b \times t_b\right)w_b \times l_p + E_b \times t_b \times w_b\left(l_b - l_p\right) \tag{2}$$

And the beam's resonance frequency f_1 is $f_1 = \frac{1}{2\pi}\sqrt{\frac{K}{M_b}}$ (3). Where K is spring constant at the point of the piezoelectric patch-Aluminium section and expressed as $K = \frac{3B_m w_b}{l_p^3}$, while B_m is the piezoelectric patch and the Aluminium section's bending modulus and computed as $B_m = \frac{w_b \times E_p^2 t_p^4 + E_b^2 t_b^4 + 2E_p E_b t_p t_b\left(2t_p^2 + 2t_b^2 + 3t_p t_b\right)}{12\left(E_p t_p + E_b t_b\right)}$.

Simultaneously, the third bending mode's vibration frequency ω is defined by $\omega = 7.855^2 \times f_1$.

Equation (4) calculates the aqueous and alcohol-based glycerol solution's viscous fluid damping f_d and is expressed as

$$f_d = 6\pi\eta r\left(1 + \frac{r}{\delta}\right) \tag{4}$$

where η—fluid's dynamic viscosity, r—the beam's depth in the test liquid, e_f—the fluid's density, δ—acoustic wave's

Fig. 2 a Piezoelectric actuated cantilever beam b Fluid's viscous drag force for aqueous-based glycerol mixture, alcohol-based glycerol mixture, aqueous-alcoholic-10% glycerol mixture
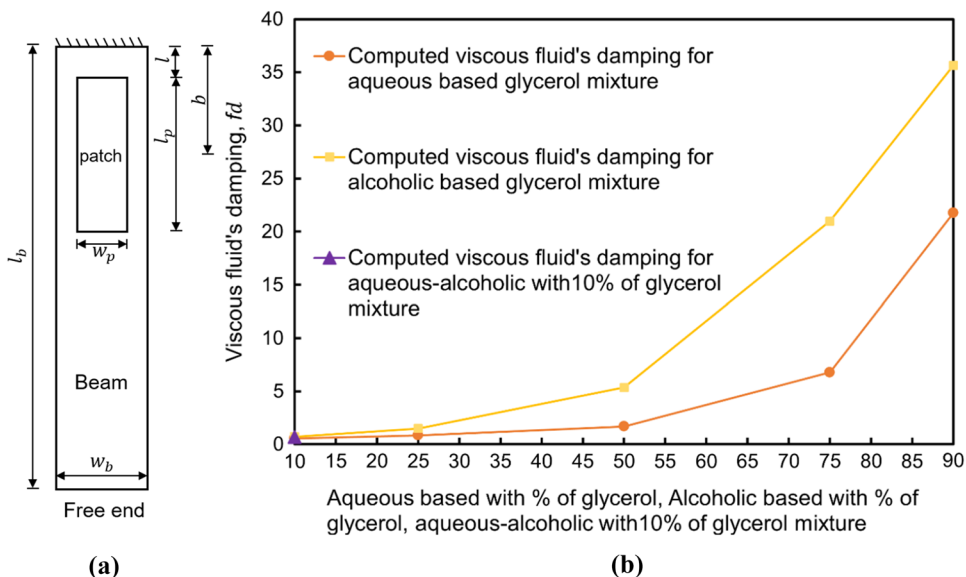
penetration depth which is computed by utilizing $\delta = \sqrt{\frac{2\eta}{\omega \rho_f}}$

.

The resultant viscous fluid's damping was computed analytically, as indicated in Fig. 2b. The aqueous-based mixture's damping was in a range of 0.5527–25.9228, whereas the alcohol-based glycerol mixture's damping was in a range of 0.7149–35.6625, which was higher than that of the aqueous-based glycerol mixture's damping. For the aqueous-alcohol − 10% glycerol solution, viscous fluid's damping was 0.6903.

Factors influencing mixture's performance

Mixture's density and viscosity

Density and viscosity are two different properties. The density of the aqueous glycerol solution differs as the concentration of glycerol changes. Andreas Volk and Christian J. Kahler developed a model to determine the density of aqueous glycerol solutions (Volk and Kähler 2018). When water mixes with glycerol, volume contraction occurs. In their work, the authors took volume contraction into account and introduced a volume contraction coefficient k, which depended on glycerol volume fraction and the solution's temperature (T). Equation (5) expresses it as

$$k\left(T, w_{gly}\right) = 1 + a sin(w_{gly}^{1.31} \pi)^{0.81} \tag{5}$$

where w_{gly}—glycerol's mass fraction,T —temperature, a—temperature-dependent coefficient determined by the equation, $a = 1.78 \times 10^{-6}T^2 - 1.82 \times 10^{-4}T + 1.41 \times 10^{-2}$.

Equation (6) calculates the aqueous glycerol solution density ρ_{mix}

$$\rho_{mix}\left(T, w_{gly}\right) = k\left(T, w_{gly}\right) \left[\rho_{wt}(T) + \frac{\rho_{gly}(T) - \rho_{wt}(T)}{1 + \frac{\rho_{gly}(T)}{\rho_{wt}(T)}\left(\frac{1}{w_{gly}} - 1\right)}\right] \tag{6}$$

where ρ_{wt} and ρ_{gly} are the densities of water and glycerol.

Similarly, another researcher Nian-Sheng Cheng, proposed a formula for glycerol–water mixture's viscosity computation for 0 – 100% glycerol concentration by mass and temperature 0 – 100 ℃ (Cheng 2008). Based on his work, water–glycerol mixture's dynamic viscosity η_{mix} is expressed by Eq. (7)

$$\eta_{mix} = \eta_{wt}^{\alpha} \eta_{gly}^{1-\alpha} \tag{7}$$

where η_{wt} and η_{gly} are the dynamic viscosities of water and glycerol. α is a weighting factor related to glycerol concentration and varies in a range 0–1 with temperature and the glycerol concentration. The weighting factor α, is represented by the equation $\alpha = \frac{ln(\mu \eta_{mix}/\eta_{gly})}{ln(\eta_{wt}/\eta_{gly})}$.

At the same time, Eq. (8) expresses α

$$\alpha = 1 - C_{gly} + \frac{ABC_{gly}\left(1 - C_{gly}\right)}{AC_{gly} + B\left(1 - C_{gly}\right)} \tag{8}$$

where C_{gly} is glycerol's concentration in terms of mass and A, B are coefficients related to the data and computed as $A = 0.705 - 0.0017T$, likewise $B = (4.9 + 0.036T)A^{2.5}$ where T is the temperature.

Equation (9) calculates glycerol's concentration C_{gly} and is expressed as

$$C_{gly} = MW_{gly}C_{mol}/\left(1000 + MW_{gly}C_{mol}\right) \tag{9}$$

where MW_{gly} corresponds to glycerol's molecular weight and C_{mol}, is the concentration of glycerol in mole fraction.

The present work measures the mixture's viscosity by an Ostwald viscometer and Eq. (10) computes viscosity (Wada 1980)

$$\eta_{mix} = \frac{\rho_{mix}t_2}{\rho_{wt}t_1}\eta_{wt} \tag{10}$$

where ρ_{wt}–DI water's density, ρ_{mix}–mixture's density, η_{wt} –DI water's viscosity, η_{mix}–mixture's dynamic viscosity, t_1 and t_2–DI water's and the mixture's flow time between two marked points separately. While measuring the viscosity of the mixture, DI water was considered as the reference fluid.

Mixture's surface tension and refractive index

Mixing of appropriate proportions of the solvent ethanol and glycerol with DI water reduces DI water's surface tension, and cleans dirt particles on hand. Hence, surface tension is an essential property for aqueous sanitizer preparation. A stalagmometer that measures surface tension consists of a capillary glass tube. The fluid drop falls from the capillary tube as the drop's weight becomes equal to the liquid's surface tension. In the present work, the drop count method computed the mixture's surface tension γ_{mix}. The equation below gives γ_{mix}

$$\gamma_{mix} = \frac{n_{wt}\rho_{mix}}{n_{mix}\rho_{wt}}\gamma_{wt} \tag{11}$$

where γ_{wt} – DI water's surface tension, n_{wt} and n_{mix}– water and mixture's drop count number, and ρ_{mix}, ρ_{wt} are the densities of the mixture and DI water correspondingly.

Likewise, the mixed solution's refractive index measurement correctly monitors its concentration, and hence, it is an important property. Refractive index is the ratio of the specified wavelength's velocity in the air to its velocity in the

fluid being considered (Takamura et al. 2012). Equation (12) represents the refractive index for aqueous glycerol solution.

$$refractive index = 1.333 w_{wt} + 1.474 w_{gly} \qquad (12)$$

where w_{wt} and w_{gly} correspond to water and glycerol weight fractions in the mixture. The present work computed the aqueous glycerol mixture's refractive index by the above equation.

Experimental setup

Figure 3a illustrates the experimental arrangement of the proposed mixing methodology. The experimental setup consists of a piezoelectrically actuated cantilever beam dipped in the test liquid. A driving unit to actuate the piezoelectric patch comprised of a function generator and a high-voltage amplifier. The measuring unit consisted of a laser displacement sensor and a DAC card. Figures 3b–f indicates a mixing tank consisting of the test liquid and a piezoelectric

actuator at rest. The test liquid could be DI water with different concentrations of glycerol. Without any driving force, there was no mixing of glycerol and DI water. Glycerol settled at the tank's bottom with a layer of DI water above it, as indicated in Figs. 3b–f. The beam's depth in the test liquid was kept constant at 5 mm, where the fluid's drag force was less.

When input excitation voltage was given to the piezoelectric actuated cantilever beam, it started to oscillate, as illustrated in Fig. 3g. Vibration energy was sent from the beam to test liquid and the mixing started. The vibrations of the piezoelectric actuated beam depend on the excitation voltage and vibration mode frequency. The piezoelectric actuated cantilever beam at the third bending mode vibration frequency produced powerful vibrations. At this mode, the fluid's influential circulation occurred vigorously in all directions, as illustrated in Fig. 3g. It resulted in strong motion of all fluid molecules, and robust mixing occurred, even at the tank's inner sidewall. In this study, the experiment was conducted at an excitation voltage of 110 V $_{P-P}$ to the piezoelectric actuator at the third bending
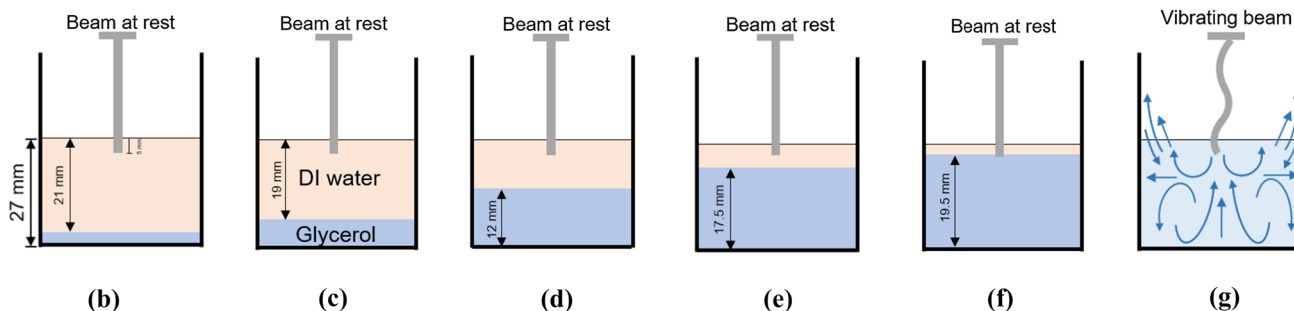

(a)

(b) **(c)** **(d)** **(e)** **(f)** **(g)**
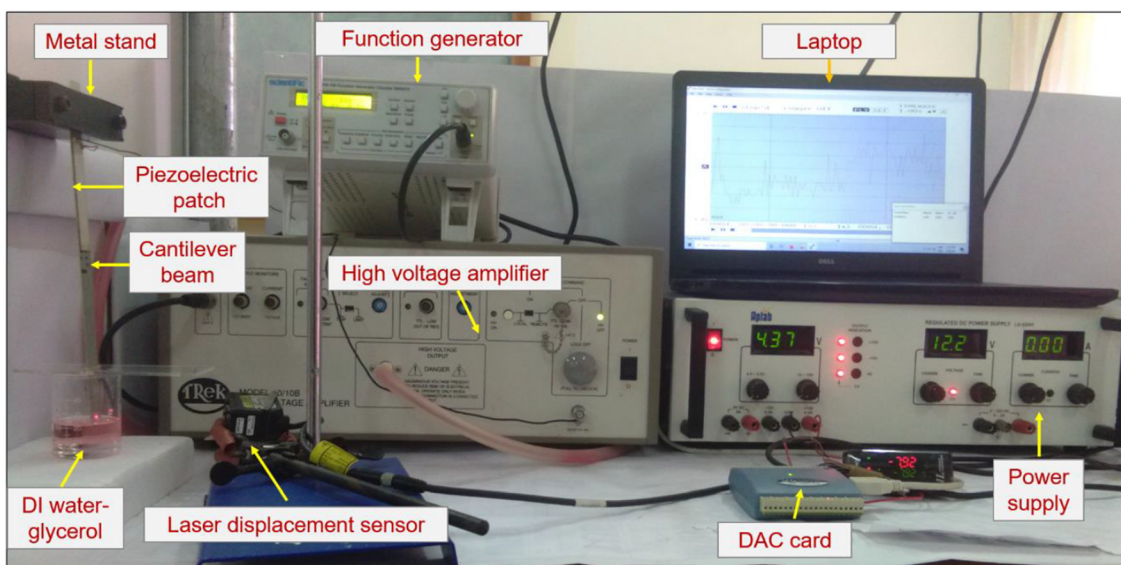
Fig. 3 **a** Experimental setup; DI water and **b** 10 **c** 25 **d** 50 **e** 75 **f** 90% glycerol **g** Vibrating beam and the mixing process

mode vibration frequency of 165.80 Hz. All mixing tests were repeated thirty times by the proposed methodology before taking the final readings in a temperature-controlled environment at 25 ℃. A stopwatch measured the time for each mixing process.

Further, the mixed solution was collected in a glass beaker to measure its density, viscosity, and surface tension and to analyse the mixing execution. Before measuring, an appropriate solvent was used to clean the piezoelectric cantilever beam's tip portion. The glass apparatus was cleansed and dried in hot air. The dye and glycerol solution's mixing execution was measured by the absorbance values and GCMS spectrum.

Results and discussion

In this study, mixing execution was validated by measuring the mixed solution's density, viscosity, surface tension and refractive index at 25 °C. The observed experimental data were compared with the analytical model and formula proposed by researchers. Table 3 and Section I show the properties of the aqueous-based mixture and Section II for the alcohol-based mixture. Section III indicates the properties of the sanitizer, which is a combination of

DI water–ethanol-10% glycerol solution. The aqueous-based mixture's measured density values were validated by the density model in (Volk and Kähler 2018) and viscosity values by the formula (Cheng 2008). Simultaneously, the aqueous-based mixture's measured experimental data, such as surface tension and refractive index, were compared with the approximate data in (Takamura et al. 2012). The alcohol-based mixture's measured surface tension data were compared with the data in (Alkindi et al. 2008).

Table 3 and Section III represent the sanitizer solution's measured parameters such as density, viscosity, and surface tension. The data consisted of six mixture samples for the same solute concentrations. The absorbance values of aqueous- and alcohol-based mixtures were measured by a UV–visible spectrophotometer and *M-17* mixture's GCMS spectrum to analyse the mixing performance, as illustrated in Table 4.

The mixture's density and viscosity analysis

Density was considered first for experimental data validation. Figure 4a shows the relation between the measured density and distinct glycerol concentrations in the aqueous mixture. The mixture's density increased with an increase in glycerol concentration. The values were in a range of

Table 3 The mixture's measured and calculated values of different properties and approximate data values provided by various researchers

I – Aqueous–glycerol's 10, 25, 50, 75, 90% concentration mixture							
Property	Unit	*M-1*	*M-2*	*M-3*	*M-4*	*M-5*	
Measured density	*g cm^{-3}*	1.0106	1.0532	1.1108	1.1970	1.2462	
Calculated density by (Volk and Kähler 2018)	*g cm^{-3}*	1.0244	1.0651	1.1366	1.2043	1.2446	
Measured viscosity	*cp*	1.1208	2.1262	6.0838	40.3409	165.6539	
Calculated viscosity by (Cheng 2008)	*cp*	1.2188	2.094	6.8559	41.295	208.13	
Measured surface tension	*dyne cm^{-1}*	69.2905	67.5137	64.351	61.7475	57.9413	
Measured refractive index	–	0.4802	0.6855	0.9883	1.2490	1.3879	
Approximate surface tension data by (Takamura et al. 2012)	*dyne cm^{-1}*	71.7	71.7	70	68.5	67.4	66.5
Mixing time	*sec*	245	268	532	724	1082	
II – Ethanol–glycerol's 10, 25, 50, 75, 90% concentration mixture							
Property	Unit	*M-6*	*M-7*	*M-8*	*M-9*	*M-10*	
Measured density	*g cm^{-3}*	0.8477	0.997	1.1021	1.1308	1.1882	
Approximate density data by (Alkindi et al. 2008)	*g cm^{-3}*	0.8508	0.9312	1.0622	1.1706	1.2268	
Measured viscosity	*cp*	1.8637	5.3164	30.490	161.2771	293.3901	
Approximate viscosity data by (Alkindi et al. 2008)	*cp*	2.4675	6.94	40.765	245.25	714.2	
Measured surface tension	*dyne cm^{-1}*	23.6683	25.8373	27.2592	30.3966	42.7632	
Approximate surface tension data by (Alkindi et al. 2008)	*dyne cm^{-1}*	22.45	23.5	27.8	37.6	50.4	
Mixing time	*sec*	252	285	568	758	1098	
III – Aqueous–ethanol–10% glycerol (Sanitizer) mixture *M-11*							
Measured density	*g cm^{-3}*	0.750384	0.7489	0.7504	0.7541	0.7484	0.7493
Measured viscosity	*cp*	1.8883	1.9325	1.8955	1.8756	1.8836	1.8681
Measured surface tension	*dyne cm^{-1}*	34.91363	34.66935	35.04868	34.6176	34.79812	34.6884
Mixing time	*sec*	260					

Table 4 Aqueous- and alcohol-based mixture's absorbance values after mixing

Aqueous-based mixture	M-12		M-13		M-14		M-15		M-16	
Wavelength nm	410	270	410	270	410	270	410	270	410	270
Absorbance	0.16	0.246	0.054	0.256	0.049	0.692	0.039	0.955	0.033	0.994
Alcohol-based mixture	M-17		M-18		M-19		M-20		M-21	
Absorbance	1.235	1.31	1.081	1.2	0.526	0.647	0.423	0.567	0.264	0.399
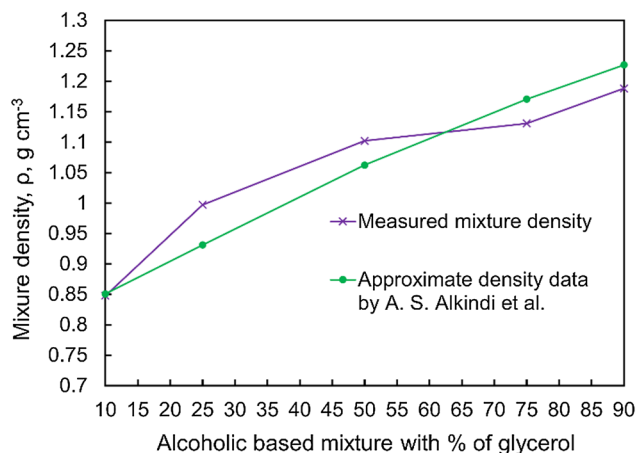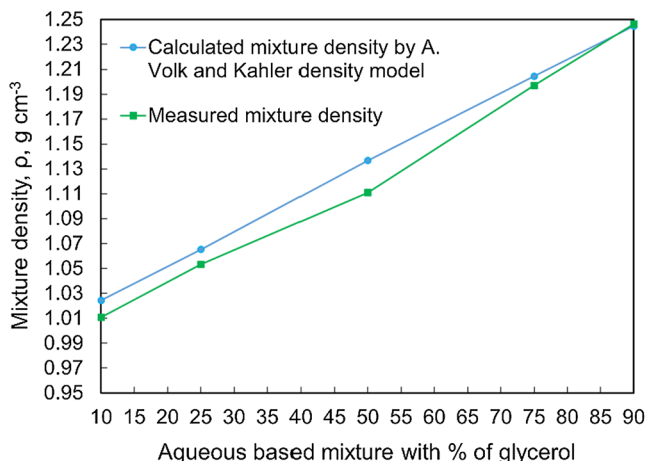
(a)

(b)
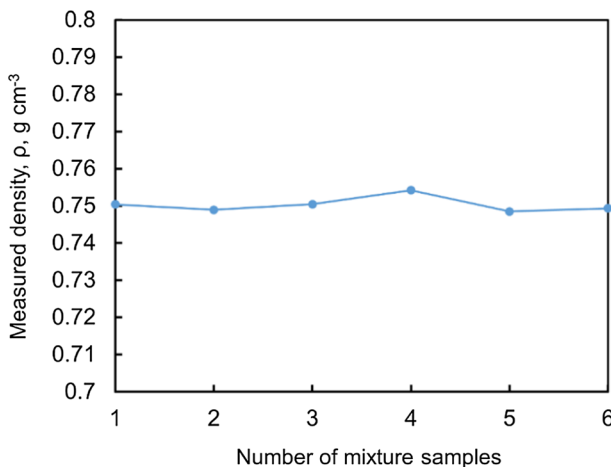
(c)

Fig. 4 Density of **a** Aqueous-based mixture with % of glycerol **b** Alcohol-based mixture with % of glycerol **c** Sanitizer solution

1.0106–1.2462 g cm^{-3}, whereas the density model's calculated density values in (Volk and Kähler 2018) were in a range of 1.0244–1.2446 g cm^{-3}. For result validation, measured and computed density values for 25% of glycerol concentration mixture were considered, and they revealed ± 1.1290% deviation. Figure 4b shows the measured densities of alcohol-based mixtures, which were compared with the approximate data provided in (Alkindi et al. 2008). Figure 4c illustrates density values for the sanitizer solution,

where six mixture samples of the same solute concentration were considered. The measured density was in a range of 0.7484–0.7541 g cm^{-3}.

Viscosity is the internal resistance measurement to fluid flow and is sensitive to temperature changes. Figure 5a shows how the measured viscosity changes with distinct glycerol concentrations in the aqueous mixture. The mixture's measured viscosity values were in a range of 1.1208–165.6539 cp, whereas the calculated values by the
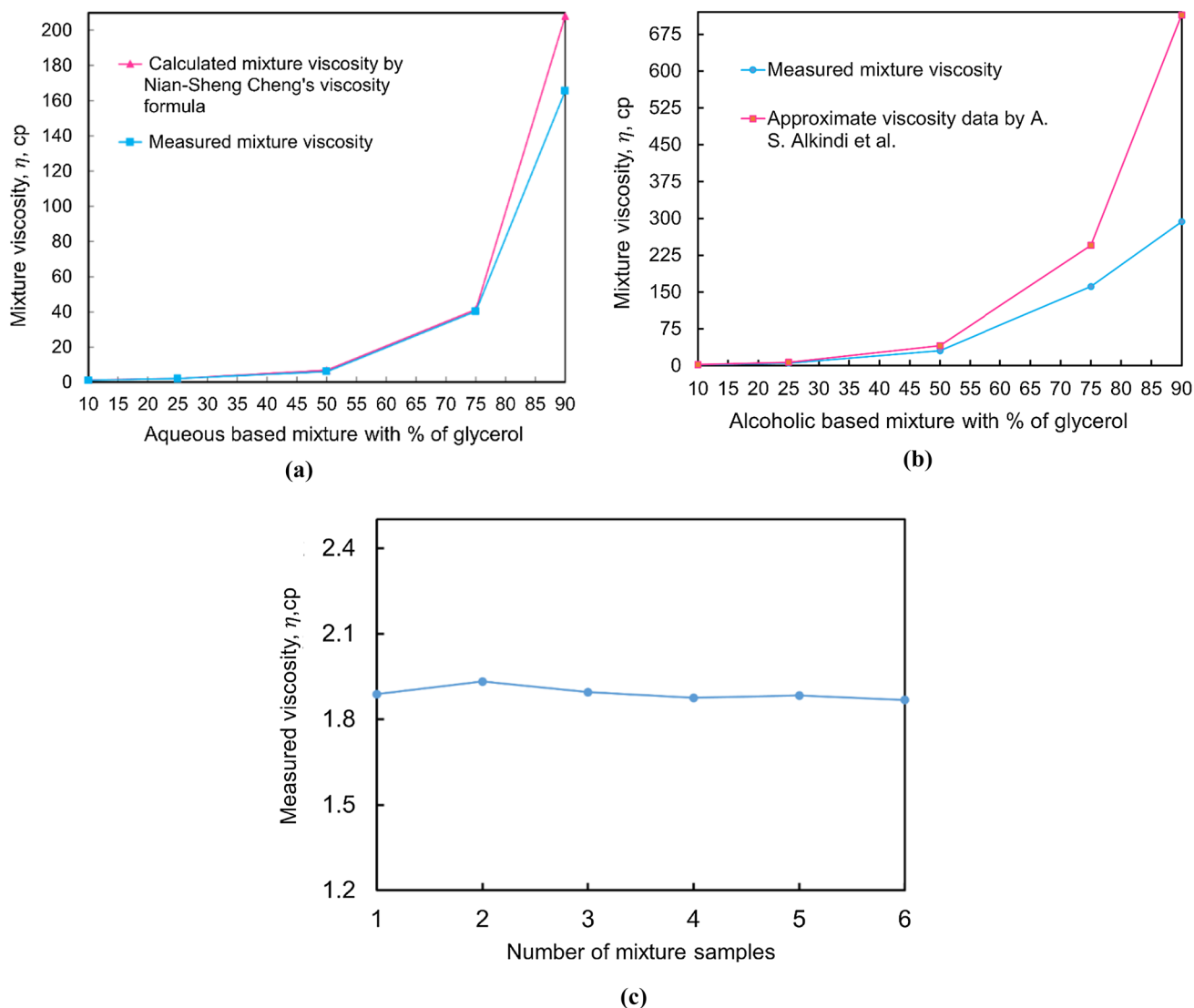
Fig. 5 Viscosity of **a** Aqueous-based mixture with % of glycerol **b** Alcohol-based mixture with % of glycerol **c** Sanitizer solution

formula in (Cheng 2008) were in the range of 1.2188–208.13 cp. For result validation, measured and computed viscosity values for 25% of glycerol concentration mixture were considered. They showed ± 1.5166% deviation. The other important observation was that the most of the measured viscosity values were below the calculated values. The piezoelectric actuator produced remarkable vibrations at the third bending mode vibration frequency resulting in better mixing by reducing the viscosity of pure glycerol. Non-uniformity in the form of viscosity decreased and the mixed solution became homogeneous. Thus, low measured viscosity values indicated better mixing performance. Figure 5b shows the alcohol-based mixture's measured viscosity which was compared with the approximate data provided in (Alkindi et al. 2008). Figure 5c indicates the sanitizer solution's viscosity values consisting of six mixture samples of the same solute

concentration, where the observed viscosity values were in a range of 1.8681–1.9325 cp.

The mixture's surface tension and refractive index analysis

The surface tension of the mixture plays a vital role in sanitizer preparation. Since an appropriate proportion of mixing the solvent ethanol and glycerol with DI water reduces DI water's surface tension, it cleans hands properly.

Figure 6a shows the surface tension of an aqueous-based, different glycerol concentration mixture. The mixture's surface tension decreased with an increase in glycerol concentration. In contrast, surface tension increased for the alcohol-based diverse glycerol concentration mixture when glycerol concentration increased, as reported in
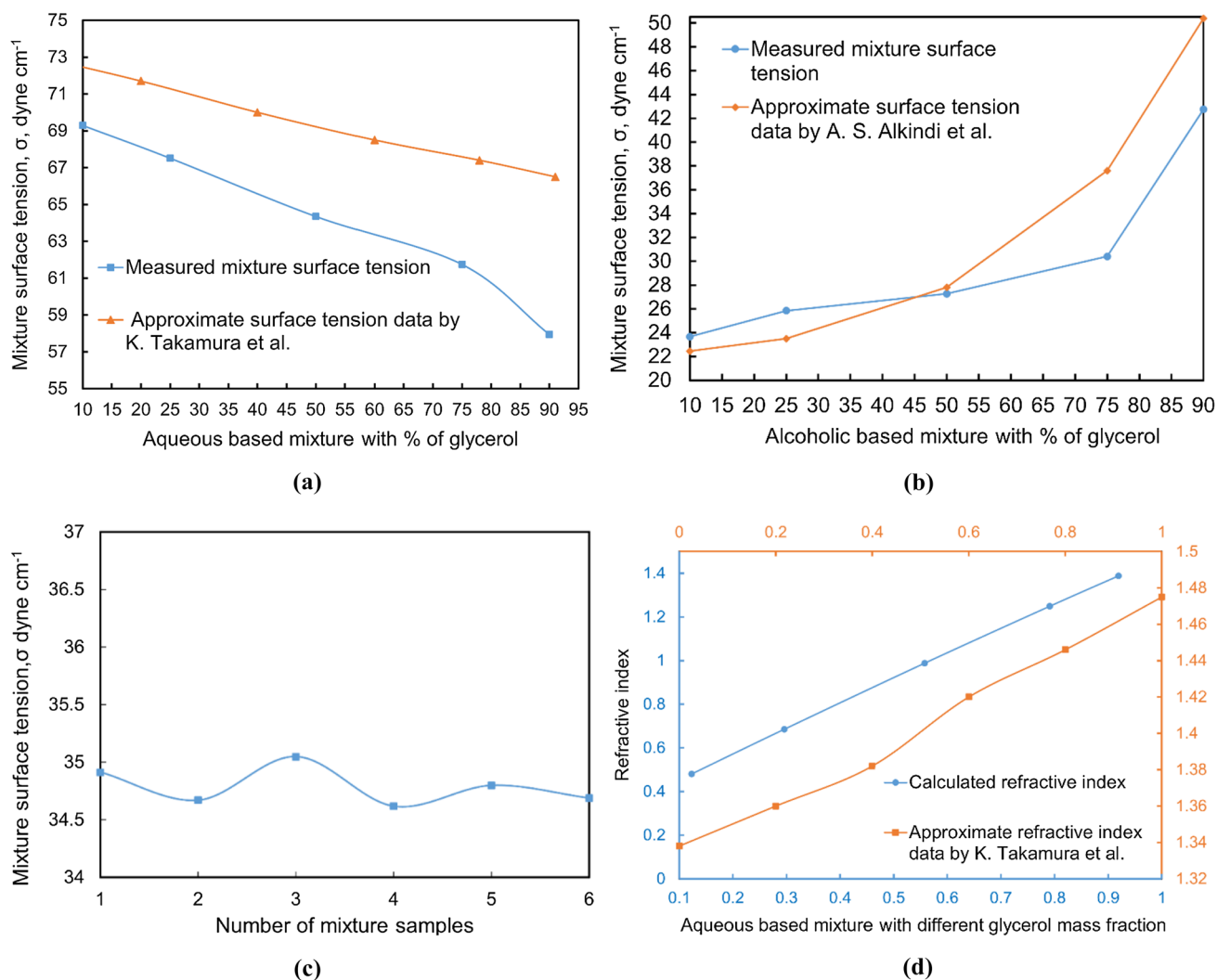
(a)

(b)

(c)

(d)

Fig. 6 Surface tension of **a** Aqueous-based mixture with % of glycerol **b** Alcohol-based mixture with % of glycerol **c** Sanitizer solution **d** Refractive index of aqueous-based mixture with different glycerol mass fractions

Fig. 6b. Figures 6a, b are a comparison of experimental surface tension data with the approximate data provided in (Takamura et al. 2012; Alkindi et al. 2008).

The sanitizer solution's surface tension was in a range of 34.6176–35.0486 dyne cm^{-1}, as documented in Fig. 6c. Similarly, the mixed solution's refractive index measurement monitored its concentration as this was essential for the mixing analysis. In this work, only the refractive index of aqueous-based different glycerol concentration mixtures was calculated by considering measured weight fraction values of water and glycerol. It is concluded from Fig. 6d that as glycerol concentration increased, the refractive index of the mixture increased correspondingly.

Mixture's absorbance values and GCMS spectrum

In addition to earlier mentioned parameters, the aqueous-based and alcohol-based mixture's mixing executions were analysed by the mixture's absorbance values measured before and after mixing. Further, the mixture preparation procedure is as mentioned in Table 2 and Sections V and VI. For the analysis, maximum absorptivity; λ_{max} values, as indicated in Table 1, were considered. The λ_{max} values for methyl red dye and glycerol were 410 and 270 nm, respectively. Absorbance values for aqueous methyl red and alcoholic methyl red dye solutions for a concentration of 10 mg l^{-1} were 0.18 and 1.318 at 410 nm before mixing. Similarly, the

absorbance numeric value for pure glycerol corresponded to 0.474 at 270 nm before mixing.

The aqueous- and alcohol-based mixture's absorbance took place in a range of 200–800 nm, as indicated in Figs. 7a, b. Whereas Table 4 demonstrates aqueous-based and alcohol-based mixture's absorbance values after mixing.

Absorbance readings for the aqueous-based mixture reduced from 0.16 to 0.033 at 410 nm and increased from 0.246 to 0.994 at 270 nm. Mixing is the process in which nonlinearity in any form, such as concentration, temperature, and phase, is reduced so that the mixed solution becomes homogeneous. In this case, the mixed solution's absorbance decreased at 410 nm and increased at 270 nm

so that the end product was homogeneous. Similarly, the alcohol-based mixture's absorbance reduced from 1.235 to 0.264 at 410 nm. However, in this case, the species formed after mixing showed that the mixture's absorbance values were also reduced from 1.31 to 0.399 at 270 nm.

Figure 7c indicates the GCMS spectrum for the mixture *M-17,* an alcoholic methyl red dye solution with a concentration of 10 mg l^{-1} mixed with 10% of glycerol. The GCMS library showed the best match for molecular weights 92 and 270, which corresponded to glycerol and methyl red dye, as illustrated in Table 1. GCMS spectrum indicated the appearance of both the constituents, methyl red dye and glycerol in the mixture.
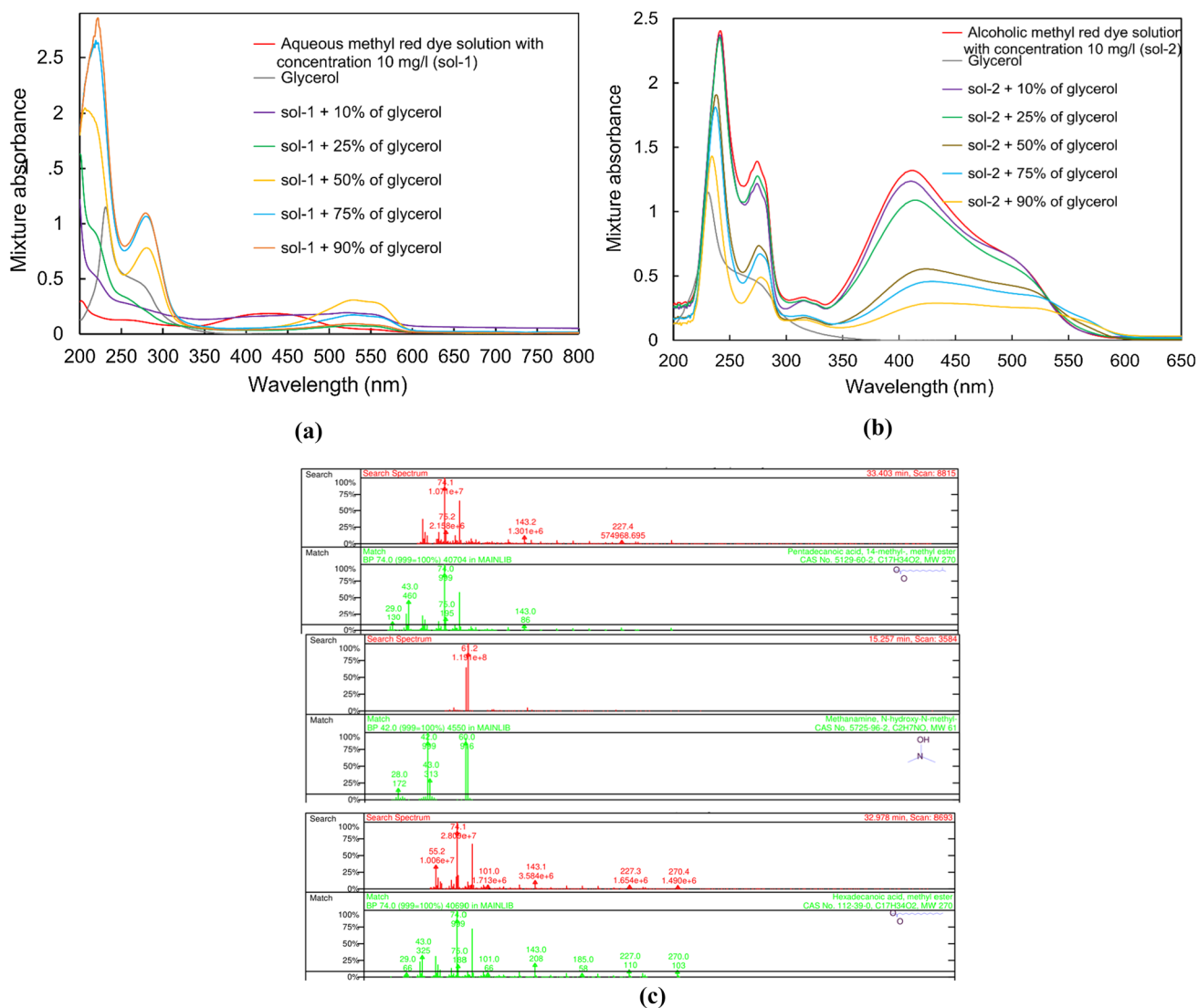

(a)

(b)

(c)

Fig. 7 Absorbance vs. wavelength for **a** Aqueous-based mixture with % of glycerol **b** Alcohol-based mixture with % of glycerol **c** GCMS spectrum for M-17 mixture

Conclusion

This study proposed a macroscopic mixer for disparate feature liquid–liquid mixing in aqueous sanitizer preparation. The proposed mixer prepared three different mixtures, namely aqueous-based glycerol, alcohol-based glycerol, and a sanitizer solution. The mixer's mixing performance evaluation was analysed by measuring the mixed solution's density, viscosity, surface tension, and refractive index. Additionally, the aqueous- and alcohol-based mixture's mixing executions were evaluated by measuring their absorbance values and GCMS spectrums.

The measured aqueous-based glycerol mixture's density and viscosity values were validated with the computed values by a prior researcher's model and formula. The observed density reading for the aqueous-based solution with 25% of glycerol concentration was in agreement with the estimated value of a density model with $\pm 1.1290\%$ deviation. Simultaneously, the measured viscosity value for 25% of glycerol concentration in the aqueous-based mixture showed $\pm 1.5166\%$ deviation with the computed value using the formula. The sanitizer mixture's measured density, viscosity, and surface tension values were 0.7502 g cm-3, 1.8906 cp, 34.7893 dyne cm^{-1}, respectively. Similarly, the GCMS spectrum for alcoholic methyl red dye mixed with 10% glycerol indicated both the constituents, methyl red dye and glycerol in the mixture. It is important to underline that the presented mixer is suitable for mixing of viscous liquids such as glycerol, honey, and different viscosity liquids. Liquid's influential circulation occurs vigorously in all directions. Hence, significant mixing occurs even at the tank's inner sidewall. Baffles are not required to improve the circulation of liquid; it happens naturally. The mixer can be actuated on demand, with size, and geometry alterations, making it ideal for micro- and large-scale applications.

Supplementary Information The online version contains supplementary material available at https://doi.org/10.1007/s11696-021-01886-3.

Declarations

Conflict of interest On behalf of all authors, the corresponding author states that there is no conflict of interest.

References

Alkindi AS, Al-Wahaibi YM, Muggeridge AH (2008) Physical properties (density, excess molar volume, viscosity, surface tension, and refractive index) of ethanol + glycerol. J Chem Eng Data 53:2793–2796. https://doi.org/10.1021/je8004479

Aubin J 2019 Advances in Mixing Research 16th European Conference on Mixing. Chem Eng Technol Doi: https://doi.org/10.1002/ceat.201970085

Aubin J, Ferrando M, Jiricny V (2010) Current methods for characterising mixing and flow in microchannels. Chem Eng Sci 65:2065–2093. https://doi.org/10.1016/j.ces.2009.12.001

Bayareh M, Ashani M N, Usefian A (2020) Active and passive micromixers: A comprehensive review. Chem. Eng. Process. - Process Intensif. 147

Bowler AL, Bakalis S, Watson NJ (2020) A review of in-line and on-line measurement techniques to monitor industrial mixing processes. Chem Eng Res Des 153:463–495. https://doi.org/10.1016/j.cherd.2019.10.045

Cai G, Xue L, Zhang H, Lin J (2017) A review on micromixers. Micromachines. https://doi.org/10.3390/mi8090274

Center for Drug Evaluation and Research (2020) Policy for Temporary Compounding of Certain Alcohol-Based Hand Sanitizer Products During the Public Health Emergency Immediately in Effect Guidance for Industry. 1–11. https://www.fda.gov/media/136118/download

Cheng NS (2008) Formula for the viscosity of a glycerol-water mixture. Ind Eng Chem Res 47:3285–3288. https://doi.org/10.1021/ie071349z

Chenlo F, Moreira R, Pereira G, Bello B (2004) Kinematic viscosity and water activity of aqueous solutions of glycerol and sodium chloride. Eur Food Res Technol 219:403–408. https://doi.org/10.1007/s00217-004-0974-6

Cristancho DM, Delgado DR, Martínez F, Mohammad A (2011) Volumetric properties of glycerol + water mixtures at several temperatures and correlation with the Jouyban-Acree model Resumen Propiedades volumétricas de mezclas glicerol + agua a varias. Rev Colomb Ciencias Químico - Farm 40:92–115

Cullen P J (2009) Food Mixing: Principles and Applications

Das SS, Tilekar SD, Wangikar SS, Patowari PK (2017) Numerical and experimental study of passive fluids mixing in micro-channels of different configurations. Microsyst Technol 23:5977–5988. https://doi.org/10.1007/s00542-017-3482-x

Dickey DS (2012) Fluid Mixing Equipment Design. Pharm Blending Mix. https://doi.org/10.1002/9781118682692.ch12

Elia B, Sandra J, Nicole R, Trevor V B (2011) Food mixing in the industrial processes https://mixing.net/food-mixing-in-the-industrial-processes/

Ghotli R A, Raman A A A, Ibrahim S, et al. (2013) LIQUID-LIQUID MIXING IN STIRRED VESSELS : A REVIEW Liquid-Liquid Mixing in Stirred Vessels : A Review. 6445. https://doi.org/10.1080/00986445.2012.717313

Hessel V, Löwe H, Schönfeld F (2005) Micromixers - A review on passive and active mixing principles. Chem Eng Sci 60:2479–2501. https://doi.org/10.1016/j.ces.2004.11.033

Kozic MS, Ristic SS, Linic SLJ et al (2016) Numerical analysis of rotational speed impact on mixing process in a horizontal twin-shaft paddle batch mixer with non-newtonian fluid. FME Trans 44:115–124. https://doi.org/10.5937/fmet1602115K

Lee J, Jing J, Yi TP et al (2020) Hand Sanitizers : A Review on Formulation Aspects, Adverse E ff ects, and Regulations. Int J Environ Res Public Health 17:3326

Lu LH, Ryu KS, Liu C (2002) A magnetic microstirrer and array for microfluidic mixing. J Microelectromechanical Syst 11:462–469. https://doi.org/10.1109/JMEMS.2002.802899

Mallinson S G, McBain G D, Horrocks G D (2016) Viscosity and surface tension of aqueous mixtures. Proc 20th Australas Fluid Mech Conf AFMC 2016 15–18

Mashimo T (2013) Piezoelectric rotational mixer based on a first bending vibration mode. IEEE Trans Ultrason Ferroelectr Freq Control 60:2098–2104. https://doi.org/10.1109/TUFFC.2013.2800

Nakagawa H, Oyama T (2019) Molecular Basis of Water Activity in Glycerol-Water Mixtures. Front Chem 7:1–9. https://doi.org/10.3389/fchem.2019.00731

Nogueira AB, Gomes WE, Sartori DS et al (2019) Determination of free glycerol in biodiesel using UV-visible spectroscopy: A validation study. Rev Virtual Quim 11:1725–1736

Ohol RM, Vasuki B (2020) Experimental Evaluation of Liquid Mixing Using Piezo Actuated Pump System. Instruments Exp Tech 63:758–766. https://doi.org/10.1134/S0020441220050206

Rahbarshahlan S, Ghaffarzadeh Bakhshayesh A, Rostamzadeh Khosroshahi A, Aligholami M (2020) Interface study of the fluids in passive micromixers by altering the geometry of inlets. Microsyst Technol. https://doi.org/10.1007/s00542-020-05067-2

Rampalli S, Dundi TM, Chandrasekhar S et al (2020) Numerical Evaluation of Liquid Mixing in a Serpentine Square Convergent-divergent Passive Micromixer. Chem Prod Process Model 15:1–11. https://doi.org/10.1515/cppm-2019-0071

Segur JB, Oderstar HE (1951) Viscosity of Glycerol and Its Aqueous Solutions. Ind Eng Chem 43:2117–2120. https://doi.org/10.1021/ie50501a040

Shankar PN, Kumar M (1994) Experimental determination of the kinematic viscosity of glycerol-water mixtures. Proc - R Soc London, A 444:573–581. https://doi.org/10.1098/rspa.1994.0039

Sharma G, Gadhiya J, Dhanawat M (2018) Textbook of Cosmetic Formulations. 51–52

Shih WY, Li X, Gu H et al (2001) Simultaneous liquid viscosity and density determination with piezoelectric unimorph cantilevers. J Appl Phys 89:1497–1505. https://doi.org/10.1063/1.1287606

Takamura K, Fischer H, Morrow NR (2012) Physical properties of aqueous glycerol solutions. J Pet Sci Eng 98–99:50–60. https://doi.org/10.1016/j.petrol.2012.09.003

Vilardi G, Verdone N (2020) Production of metallic iron nanoparticles in a baffled stirred tank reactor: Optimization via computational fluid dynamics simulation. Particuology 52:83–96. https://doi.org/10.1016/j.partic.2019.12.005

Vilardi G, Stoller M, Palma LD et al (2019) Metallic iron nanoparticles intensified production by spinning disk reactor: Optimization and fluid dynamics modelling. Chem Eng Process 146:107683. https://doi.org/10.1016/j.cep.2019.107683

Vilardi G, Caprariis BD, Stoller M et al (2020) Intensified water denitrification by means of a spinning disk reactor and stirred tank in series: Kinetic modelling and computational fluid dynamics. Journal of Water Process Engineering 34:101147. https://doi.org/10.1016/j.jwpe.2020.101147

Volk A, Kähler CJ (2018) Density model for aqueous glycerol solutions. Exp Fluids 59:1–4. https://doi.org/10.1007/s00348-018-2527-y

Wada Y (1980) Viscosity of liquids. J Japan Soc Lubr Engr. https://doi.org/10.1201/9781482277425-63

Wegner J, Ceylan S, Kirschning A (2011) Ten key issues in modern flow chemistry. Chem Commun 47:4583–4592. https://doi.org/10.1039/c0cc05060a

Williams AM, Griffiths DJ, Vlachos PP (2009) Sensors and Actuators A : Physical Laminar Mixing Using Oscillating Cantilevered Ionic Polymer Actuators 153:105–113. https://doi.org/10.1016/j.sna.2009.04.028

Zhang Z, Chen G (2008) Liquid mixing enhancement by chaotic perturbations in stirred tanks. Chaos, Solitons Fractals 36:144–149. https://doi.org/10.1016/j.chaos.2006.06.024

Zhang C, Siegel S H, Yenuganti S et al (2019) Sensitivity analysis of piezo-driven stepped cantilever beams for simultaneous viscosity and density measurement. Smart Mater Struct 28:065012. https://doi.org/10.1088/1361-665X/ab1706

Zhu Y, Shum P, Lu C et al (2003) Measurements of Glycerine Concentration in Water Solution by Using Long-Period Grating Refractometer. Proc IEEE Sensors 2:409–411. https://doi.org/10.1109/icsens.2003.1278969